Aharonov-Bohm phase shift in an open electron resonator

D. S. Duncan, M. A. Topinka, and R. M. Westervelt
Division of Engineering and Applied Sciences and Department of Physics, Harvard University, Cambridge, Massachusetts 02138

K. D. Maranowski and A. C. Gossard
Materials Department, University of California Santa Barbara, Santa Barbara, California 93106

(Received 3 January 2001; published 25 June 2001)

Magnetoconductance measurements are presented for open electron resonators fabricated in a $GaAs/Al_xGa_{1-x}As$ heterostructure. Conductance peaks in the transport signal are observed, which are explained by the constructive interference of electron waves with the Fermi wavelength. The application of a perpendicular magnetic field causes a shift in the peak positions, which is explained by the combined effects of electron trajectory bending and the Aharanov-Bohm phase shift.

DOI: 10.1103/PhysRevB.64.033310 PACS number(s): 73.23.−b, 73.23.Ad

An electron resonator is an open cavity in a two-dimensional electron gas (2DEG) heterostructure into which electrons can be injected via a quantum point contact.[1] Transport through the resonator is ballistic and may be characterized by a semiclassical picture in which electrons carry phase while moving along classical trajectories, analogous to light rays in geometrical optics. For this reason, the resonator falls under the rubric of ''electron optics'' devices.[2,3] In previous work, transport measurements on resonators revealed a striking series of conductance peaks occurring each time the resonator cavity length changed by $\lambda_f/2$, where λ_f was the 2DEG Fermi wavelength.[1] This behavior was explained by the constructive interference of backscattered electron waves at the point contact position each time the path length of their trajectories changed by λ_f, similar to an optical Fabry-Pérot interferometer. Theoretical work explained these observations and predicted further fine structure in the resonator conductance properties.[1,4]

In this paper we present magnetoconductance measurements on an electron resonator, which provide further insight into electron transport in these devices. The dependence of the resonator conductance peaks on a perpendicular magnetic field was studied, and a dramatic shift in the peak positions occurred as the magnetic field was increased. This shift is explained by the combined effects of electron trajectory bending by the magnetic field and the Aharonov-Bohm (AB) phase shift. The latter contribution is shown to be essential to explain the observed data. Previous manifestations of the AB phase shift in mesoscopic structures have been observed in devices in which the two paths by which electrons traverse the device are defined by microfabrication.[5–9] In contrast, our measurements rely only on the ballistic motion of electrons inside a simply connected structure to observe the AB phase shift, and thus constitute an unusual observation of the AB phase shift in an open mesoscopic system.

Figure 1(a) is a scanning electron microscope photograph of the electron resonator, which consists of a single quantum point contact (QPC) and a cylindrical reflecting mirror, formed by gates on the surface of a $GaAs/Al_xGa_{1-x}As$ heterostructure using electron-beam lithography and Cr-Au metallization. The heterostructure contains a 2DEG located 57 nm beneath the surface with a mobility 450 000 $cm^2/V\,s$ and sheet density $3\times10^{11}/cm^2$; the corresponding Fermi wavelength is 46 nm. The size of the resonator cavity is varied by changing the voltage V_g on the reflecting gate. The radius of curvature of the reflecting gate is 800 nm, and at depletion the focal point of the reflector arc lies at the QPC center. This geometry causes electron waves injected through the QPC to be reflected back towards the QPC; electrons can undergo many reflections within the cavity before

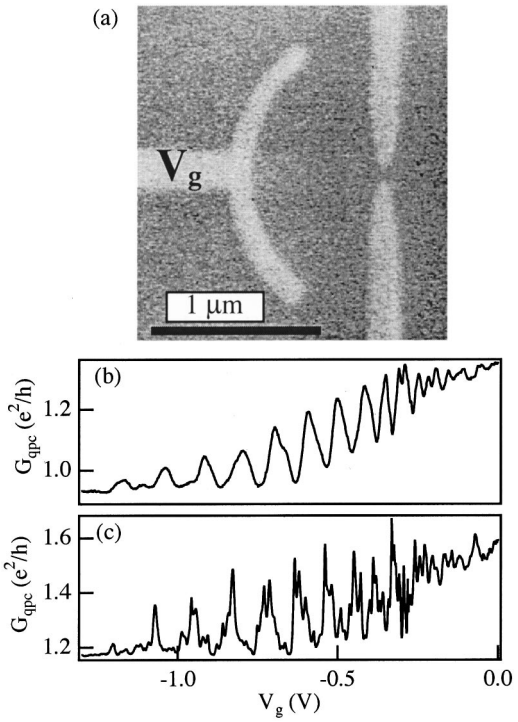

FIG. 1. (a) Scanning electron microscope photograph of an electron resonator device, consisting of a single quantum point contact and a cylindrical reflector, defined by gates in a 2DEG heterostructure. The resonator gate voltage V_g determines the size of the cavity. (b) Measured differential conductance through the point contact vs V_g at 500 mK. After depletion, a series of periodic conductance peaks is observed caused by constructive interference of electron waves at the point contact. (c) Similar measurement at dilution refrigerator temperature 25 mK, showing additional fine structure.

they escape through the open sides of the resonator. Ohmic contacts to the 2DEG are located outside of the cavity on both sides of the QPC. Standard lockin techniques were used to measure the conductance G_{QPC} through the QPC as V_g and magnetic field B were varied. All measurements were done in a dilution refrigerator at temperatures ranging from a base temperature of 25 to 500 mK.

Figures 1(b) and 1(c) demonstrate the operation of the resonator. These graphs show the differential conductance through the point contact G_{QPC} vs V_g at dilution refrigerator temperatures of (b) 500 mK and (c) 25 mK. For these measurements, the QPC was first tuned to the tunneling regime. In Fig. 1(b), peaks in G_{QPC} are observed after depletion beneath the reflecting gate at $V_g \sim -0.3\,\mathrm{V}$. The spacing between peaks increases as V_g becomes more negative due to the nonlinear mapping between V_g and the position of the reflector electrostatic boundary. These peaks are associated with the simplest electron trajectories, which emanate straight out from the QPC and are reflected straight back, and occur each time the path length of these trajectories changes by λ_f. Figure 1(c) shows fine-structure modulating the primary peaks, which occurs at lower temperatures. Such secondary structure has been associated with more complex electron trajectories and modes within the resonator.[1] The fine structure varies between different resonators and thermal cycles but is reproducible for a given device for a given cooldown. At higher temperatures, thermal smearing washes out the fine structure and only the primary peaks are resolvable. The primary peaks are a robust effect, and were observed in six different resonator devices.

Figure 2 shows the principal result of this paper, the magnetic-field dependence of the resonator conductance peaks. Figure 2(a) shows the differential conductance through a resonator for zero dc voltage as a function of reflecting gate voltage V_g and the magnetic-field B applied perpendicular to the plane of the 2DEG, taken at a dilution refrigerator temperature of 25 mK. Light regions correspond to high conductance, dark regions to low. At $B=0$ T, a series of primary conductance peaks modulated by finer, secondary peaks is observed. As B is increased, the most striking effect observed is a downward curvature in the conductance peak positions, i.e., a phase shift in the peak positions. The curvature is slight at first, but becomes more pronounced at higher magnetic fields. The curvature varies with magnetic field, but is approximately the same for all conductance peaks at a given field value. Figure 2(b) shows data from an identical measurement on a different resonator device, demonstrating the reproducibility of the overall conductance peak motion. Similar phase shifts in the conductance peak positions with B were observed in three different resonator devices.

To explain the shift in conductance peak positions, we first consider the bending of electron trajectories by the magnetic field. The electron path we consider is the simple straight out and back path responsible for the primary conductance peaks, depicted in Fig. 3(a). These linear segments are bent by a magnetic field into arcs with a radius of curvature given by the cyclotron radius r_c:

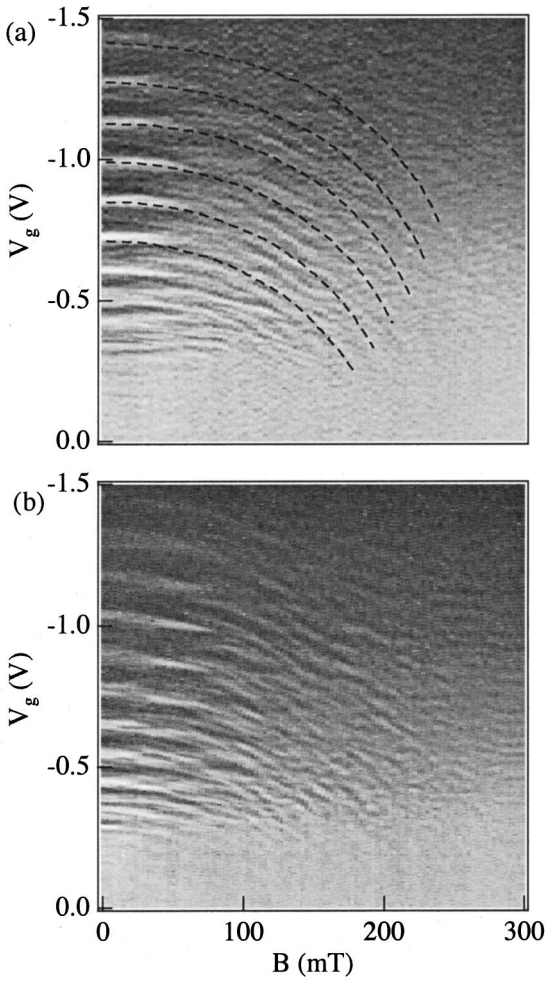

FIG. 2. (a) Measured differential conductance through the resonator, indicated by gray scale, as a function of reflector gate voltage V_g and magnetic field B. At $B=0$ T, a series of conductance peaks is observed. As B is raised, the peak positions curve downward. Dashed lines are from the calculation of Fig. 4(a). (b) Identical measurement using a different electron resonator device.

$$r_c = \frac{m^* v_f}{eB},$$

where $m^* = 0.067\, m_e$ is the effective mass of electrons in GaAs and $v_f = 2.5 \times 10^7$ cm/s is the Fermi velocity of electrons in this heterostructure. This bending, shown in Fig. 3(b), changes the path length of electron trajectories; thus the combination of magnetic-field and reflector gate position determines the overall path length. The change in path length Δl for a reflector distance y is given by

$$\Delta l = 4 r_c \ \arcsin\left(\frac{y}{2r_c}\right) - 2y.$$

In general, increasing the magnetic field increases path lengths. With this mechanism only, conductance peak positions would shift upward in Fig. 2 as the field is increased, because the cavity size must decrease to compensate for the effect of the magnetic field. This is in contradiction to the data of Fig. 2(a) and Fig. 2(b).

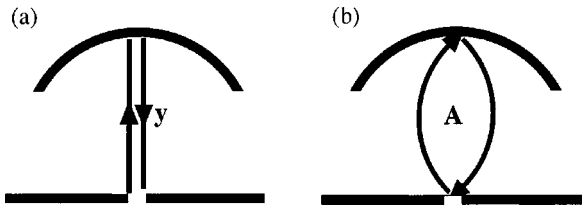

FIG. 3. (a) Schematic diagram illustrating backscattering of electron trajectories responsible for primary conductance peaks at $B=0$ T. (b) A finite magnetic field B bends straight trajectories into arcs with a radius of curvature equal to the cyclotron radius. Backscattered trajectories enclose an area A.

To explain our data, we must introduce the Aharonov-Bohm contribution to the phase in our calculation. As the linear trajectories are bent into arcs by the magnetic field, the electron path encloses an area A that increases with magnetic field, as indicated in Fig. 3(b). This area is given by

$$A(r_c)=r_c^2\left[\theta-2\cos\left(\frac{\theta}{2}\right)\sin\left(\frac{\theta}{2}\right)\right]$$

with

$$\theta=2\arcsin\left(\frac{y}{2r_c}\right).$$

The flux enclosed by this area is the product of A and the magnetic field; the number of flux quanta threading A determines the Aharonov-Bohm phase shift.

The net effect of the path length change due to trajectory bending and the Aharonov-Bohm shift Δ_{AB} is determined by calculating the total phase accumulated in a roundtrip path. This is given by

$$\phi_{\text{total}}=2\pi\left(\frac{2r_c\theta}{\lambda_f}-\frac{A(r_c)B}{\Phi_0}\right),$$

where $\Phi_0=4.14\times10^{15}\,\text{T m}^2$ is the flux quantum. In Fig. 4(a) this expression is plotted (modulo 2π) for electron reflector distances ranging from 600 to 800 nm, and for magnetic-field values ranging from 0 to 300 mT. Only lines of constant phase, corresponding to conductance peak positions, are plotted. The x and y axes scales have been chosen to correspond to Fig. 2. The calculation of Fig. 4(a) has been used to plot the dashed lines in Fig. 2(a). This calculation reproduces the overall peak motion very well, especially in the regime of smaller cavity sizes, where the effect of V_g on the cavity size is approximately linear. No adjustable parameters were used for these calculations.

To illustrate the necessity to including the Aharonov-Bohm contribution to the phase shift, Fig. 4(b) plots the total phase accumulated solely due to path length changes induced by the magnetic-field trajectory bending, i.e., without the

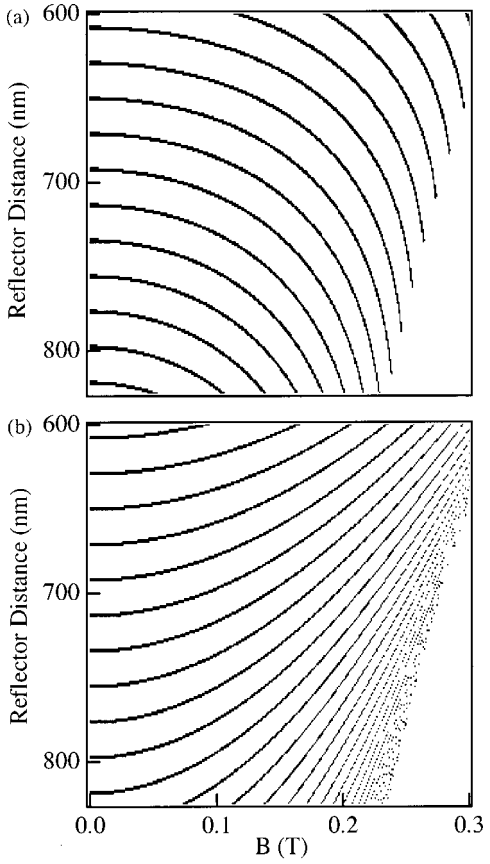

FIG. 4. (a) Calculated lines of constant phase accumulated on backscattered electron trajectories illustrated in Fig. 3 vs reflector gate position and magnetic field B. Lines of constant phase correspond to conductance peak positions. Total phase is the geometric contribution due to trajectory bending plus the AB contribution. These lines reproduce the peak motion observed in the data. (b) Same plot as (a), but for the geometric contribution only. Lines evolve in the opposite direction, indicating the need to consider the AB contribution.

Aharonov-Bohm phase shift. The same x and y axes were used as for Fig. 4(a). In this case, the lines of constant phase evolve upward as the field is raised. This is in the opposite direction as in Fig. 2, but in agreement with the qualitative argument given earlier. Thus, it is essential to include the Aharonov-Bohm contribution in the calculation. These data constitute an unusual observation of the Aharonov-Bohm phase shift in an open system.

We thank E. Heller for valuable discussions. This work was supported at Harvard by ONR Grant No. N00014-99-1-0347, NSF Grant No. NSF DMR-98-0-2242, the MRSEC program of the NSF under Award No. DMR-98-09363, and at UCSB by QUEST, an NSF Science and Technology Center.

[1] J. A. Katine, M. A. Eriksson, A. S. Adourian, R. M. Westervelt, J. D. Edwards, A. Lupu-Sax, E. J. Heller, K. L. Campman, and A. C. Gossard, Phys. Rev. Lett. **79**, 4806 (1997).
[2] J. Spector, H. L. Stormer, K. W. Baldwin, L. N. Pfeiffer, and K. W. West, Appl. Phys. Lett. **56**, 967 (1990).
[3] J. Spector, H. L. Stormer, K. W. Baldwin, L. N. Pfeiffer, and K. W. West, Appl. Phys. Lett. **56**, 1290 (1990).
[4] J. D. Edwards, M. R. Haggerty, and E. J. Heller (unpublished).
[5] E. Buks, R. Schuster, M. Heiblum, D. Mahalu, V. Umansky, and H. Shtrikman, Phys. Rev. Lett. **77**, 4664 (1996).
[6] R. Schuster, E. Buks, M. Heiblum, D. Mahalu, V. Umansky, and H. Shtrikman, Nature (London) **385**, 417 (1997).
[7] I. L. Aleiner, N. S. Wingreen, and Y. Meir, Phys. Rev. Lett. **79**, 3740 (1997).
[8] S. Washburn and R. A. Webb, Adv. Phys. **35**, 375 (1986).
[9] A. Yacoby, M. Heiblum, V. Umansky, H. Shtrikman, and D. Mahalu, Phys. Rev. Lett. **73**, 3149 (1994).